Bull. Chem. Soc. Jpn., **70**, 2703—2708 (1997)

Mixed-Valence Ruthenium Diphosphates with a Tunnel Structure: $ARu_2(P_2O_7)_2$ (A = Li, Na, Ag, and Cu) and $Ru_2(P_2O_7)_2$

Hiroshi Fukuoka,[*,#] **and Hideo Imoto**

Department of Chemistry, School of Science, The University of Tokyo, Hongo, Bunkyo-ku, Tokyo 113

(Received May 23, 1997)

Mixed-valence ruthenium diphosphates with a tunnel structure, $ARu_2(P_2O_7)_2$ (A=Li, Na, Ag, and Cu), were prepared by the reaction of an amorphous ruthenium phosphate, $H_2RuP_3O_{10}$, with Li_2CO_3, $NaNO_3$, $AgNO_3$, and $Cu_3(PO_4)_2{\cdot}3H_2O$, respectively. The structure has a three-dimensional network constructed with RuO_6 and P_2O_7 groups, and has large tunnels where A cations reside. In the sodium system, two isotypic compounds were obtained. One was obtained as single crystals and the X-ray structure analysis showed ruthenium and sodium vacancies. Another was obtained as powder and Rietveld analysis did not indicate ruthenium vacancies. It is paramagnetic and shows an antiferromagnetic transition at around 5.5 K. The phosphate with no cation in the tunnel, $Ru_2(P_2O_7)_2$, was obtained as a powder upon heating amorphous ruthenium phosphate (atomic ratio P/Ru is ≅ 4).

In our recent studies of the Ru–P–O system, three ruthenium phosphates were discovered.[1] They were two types of polyphosphates ($Ru(PO_3)_3$) and one *cyclo*-hexaphosphate ($Ru_2P_6O_{18}$). A ruthenium silicophosphate ($RuSiP_3O_{11}$) was also reported.[2] All of the phosphates contained only Ru(III) ions, in contrast with the solid-state oxides, where Ru(IV) and Ru(V) ions are common. In the present study, we introduced monovalent and divalent cations to the Ru–P–O system and obtained a new type of ruthenium phosphate containing Ru(IV) ions.

The new ruthenium phosphates are isotypic with $AM_2(P_2O_7)_2$-type compounds (A = Na, M = Mo; A = Sr, M = V).[3—5] These compounds contain parallel tunnels where A cations reside and their frameworks are built up from isolated MO_6 octahedra and P_2O_7 groups. The molybdenum analog containing monovalent cations in the tunnels has two kinds of molybdenum sites, M1 and M2, which are occupied by Mo(IV) and Mo(III) ions, respectively. On the other hand, in the vanadium phosphate with divalent cations in the tunnel, both metal sites are occupied by V(III) ions. These observations imply that the $AM_2(P_2O_7)_2$ structure has the ability to take monovalent or divalent cations in the tunnel by changing the oxidation state of the transition metal ions. In the present paper we describe the syntheses of ruthenium analogs with various cations in the tunnel.

Experimental

Polycrystalline products were identified by the powder XRD analysis. The lattice parameters of these samples were determined by a least-squares method. $H_2RuP_3O_{10}$ (**1**) was prepared as described before.[1]

Preparation of $NaRu_2(P_2O_7)_2$ (2). A mixture of **1** and $NaNO_3$ in a mole ratio of Na/Ru = 0.5 was heated at 650 °C for 1 week and then at 950 °C for 1 week. A dark-brown powder of **2** was obtained as a single phase.

Preparation of Single Crystals of $Na_{0.88}Ru_{1.75}(P_2O_7)_2$ (3). A mixture of **1** and $NaNO_3$ in a mole ratio of Na/Ru = 0.5 was heated at 500 °C for 2 d and pressed into pellets. The pellets were wrapped in a gold foil and sealed in an evacuated silica ampoule. It was heated at 910 °C for 1 week and a few black single crystals of **3**, other ruthenium phosphates, and ruthenium dioxide were obtained. The composition of **3** was determined from the single crystal X-ray analysis.

Preparation of $LiRu_2(P_2O_7)_2$ (4). A mixture of **1** and Li_2CO_3 in a mole ratio of Li/Ru = 1.04 was heated under N_2 gas at 600—700 °C, and a dark-brown powder was obtained. Powder XRD showed that the product was a mixture of **4** and $Ru(PO_3)_3$ (monoclinic). If an equivalent amount of lithium carbonate (Li/Ru = 0.5) was used, **4** was not yielded as the main product.

Preparation of $AgRu_2(P_2O_7)_2$ (5). A mixture of **1** and $AgNO_3$ in a mole ratio of Ag/Ru = 0.5 was heated under N_2 gas at 700 °C for 1 week, and a dark-brown powder was obtained. Powder XRD showed that the powder contained **5** and $Ru(PO_3)_3$ (monoclinic).

Preparation of $CuRu_2(P_2O_7)_2$ (6). A mixture of **1** and $Cu_3(PO_4)_2{\cdot}3H_2O$ in a mole ratio of Cu/Ru = 0.8 was heated at 640—800 °C for 1 week. Powder XRD indicated that the reaction yielded a mixture of **6**, $Ru(PO_3)_3$ (monoclinic), and $Cu_2P_2O_7$. Although we tried other copper sources such as $CuCl_2{\cdot}2H_2O$, $Cu(OH)_2$, $Cu(NO_3)_2{\cdot}3H_2O$, and CuO, none of the reactions with these copper sources yielded any **6**.

Preparation of [ ]$Ru_2(P_2O_7)_2$ (7). An amorphous ruthenium phosphate different from 1 was prepared by heating a mixture of ruthenium chloride hydrate and phosphoric acid in a mole ratio of Ru : P = 1 : 4 at 350 °C for 1 week. The X-ray fluorescence analysis showed that the ratio of Ru : P was 1 : 4. Heating the amorphous phosphate in a sealed silica ampoule at 870 °C for 4 d yielded a mixture of $Ru(PO_3)_3$ (monoclinic) and a compound isotypic with **2**. Because no cation that could enter the tunnels was added in the reaction system, the latter compound was identified to be [ ]-$Ru_2(P_2O_7)_2$ (**7**), where [ ] means the vacancy.

Rietveld Analysis of 2. Powder diffraction measurements of

Present address: Department of Applied Chemistry, Faculty of Engineering, Hiroshima University, Higashi-Hiroshima 739, Japan.

a polycrystalline sample of **2** were made on a Rigaku Geiger-Flex RAD-C diffractometer equipped with a counter-side monochromator using Cu $K\alpha$ radiation. The data for the analysis were collected in the step-scan mode (0.04° step) up to 120°. The total-pattern-fit program RIETAN[6)] was used in the refinement of structural parameters. The atomic coordinates of $NaMo_2(P_2O_7)_2$[3)] were used as initial parameters. An isotropic thermal parameter was refined for each kind of atom.

Single Crystal X-Ray Analysis of 3. A single crystal with dimensions $0.07\times0.05\times0.02$ mm was obtained by cutting a large polycrystalline piece with a razor blade. Intensity data collection was performed by a Rigaku AFC5R diffractometer using monochromatized Mo $K\alpha$ radiation. Intensity data were empirically corrected for absorption.[7)] The structure was solved using the initial parameters of **2**, and refined by a full-matrix least-squares refinement (ANYBLK[8)]). When only sodium atoms had deficiency, the final reliability factors were $R=6.97\%$ and $R_W=6.98\%$ for 104 variables. On the other hand, by a refinement in which the occupational factors of Ru and Na were not fixed, the calculation converged into $R=5.8\%$ and $R=5.0\%$ for 106 variables. Because the R values were much lower in the latter refinement, we concluded that the crystal had ruthenium and sodium deficiencies. The detailed crystallographic data and the complete F_o-F_c table are deposited as Document No. 70041 at the Office of the Editor of Bull. Chem. Soc. Jpn.

Magnetic Susceptibility Measurement. The magnetic susceptibility measurements of **2** were carried out by using a Faraday balance (Institute for Molecular Science). The measurement system was equipped with an Oxford magnetometer and a Cahn balance supported by original computer programs for measurements and analysis.[9)] A polycrystalline sample of **2** was contained in a silica basket and covered with cotton thread. The magnetic-field dependence curve was almost linear up to 30 kOe at 4 K. The temperature dependence curve was measured at 10 kOe (main field) and 500 Oe cm^{-1} (gradient field). A correction for the susceptibility of the basket and cotton was made prior to the measurements. The diamagnetism from all atoms ($\chi_{dia}=-3.508\times10^{-7}$ cgs·emu g^{-1}) in $NaRu_2(P_2O_7)_2$ was calculated from the reported values.[10,11)]

Results and Discussion

Preparation. The amorphous ruthenium phosphate **1** is a key compound for preparing tunnel compounds **2**—**6**. When a mixture of ruthenium chloride, phosphoric acid, and alkali or copper source was heated, the tunnel compound was not obtained at all, or was obtained as only a minor product. We could obtain the pure phase of the tunnel compound only in the Na–Ru–P–O system. The difficulty of obtaining pure compounds of **4**—**6** is related to their thermal instability. Although compound **2** is stable up to 1000 °C in an inert atmosphere, other compounds, **4**—**6**, decomposed below 950 °C.

Compound **7** is isotypic with other phosphates, **2**—**6**, but has no cation in the tunnels. It is denoted by the formula [ ]$Ru_2(P_2O_7)_2$ (**7**), where [ ] means vacancies of the A site. This phosphate is a compound of tetravalent ruthenium. The lattice parameters of **2**—**7** are listed in Table 1 with those of molybdenum and vanadium analogs.

Powder Sample of $NaRu_2(P_2O_7)_2$ (2). The Rietveld analysis showed that **2** is isotypic with $AM_2(P_2O_7)_2$ (A = Na, M = Mo; A = Sr, M = V). Its space group is triclinic $P\bar{1}$ and the refined cell constants are $a=4.7802(2)$, $b=6.9797(2)$, $c=7.9179(2)$ Å, $\alpha=91.170(2)°$, $\beta=92.192(2)°$, and $\gamma=106.784(2)°$. Since some deficiency of the sodium atom had been mentioned for the molybdenum analog,[3)] the occupational parameters of sodium and ruthenium atoms were refined, but the results showed no vacancy in their sites. In the final refinement, their occupations were fixed at the full occupancies. The results of the Rietveld analysis are presented in Fig. 1, and the refined atomic parameters and selected interatomic distances are listed in Tables 2 and 3. The crystal structure shown in Fig. 2 has large tunnels running along the a-axis where sodium ions are situated. The framework has an interconnection of RuO_6 octahedra and diphosphate ions. The average oxidation state of ruthenium is +3.5 and this phosphate is a mixed-valence compound containing equal amounts of Ru^{3+} and Ru^{4+}. These ions occupy two different crystallographic sites, (0.5, 0, 0.5) for Ru1 and (0, 0.5, 0) for Ru2, and each position is on an inversion center. The average bond length of Ru–O is 1.98 Å for Ru1 and 2.02 Å for Ru2. Taking their standard deviations into account, it is not very certain whether the average Ru–O distance is significantly longer for the Ru2 site than for the Ru1 site. However, in the isotypic molybdenum compound $NaMo_2(P_2O_7)_2$, both of the two reported structure determinations showed that the Mo(1)–O distances were clearly shorter than the Mo(2)–O distances, and it was suggested that the Mo1 sites were occupied by tetravalent metal atoms.[3,4)] Because the molybdenum and ruthenium analogues have very similar structures, it is probable that the Ru1 site, which corresponds to the Mo(1) site, is occupied by Ru(IV). The positions of sodium ions

Table 1. Lattice Constants of $ARu_2(P_2O_7)_2$ and Isotypic Compounds with Other Transition Metals

Sample name	a (Å)	b (Å)	c (Å)	α (°)	β (°)	γ (°)	V (Å^3)	
$Ru_2(P_2O_7)_2$[a)]	(4.726)	(6.825)	(7.940)	(91.62)	(92.83)	(106.7)	(244.8)	**7**
$Na_{0.88}Ru_{1.75}(P_2O_7)_2$	4.7384(8)	6.842(1)	7.953(3)	90.72(2)	92.74(2)	105.60(1)	248.0(1)	**3**
$NaRu_2(P_2O_7)_2$	4.7802(2)	6.9797(2)	7.9179(2)	91.170(2)	92.192(2)	106.784(2)	252.60(2)	**2**
$LiRu_2(P_2O_7)_2$	4.799(4)	6.954(9)	8.003(6)	92.72(6)	93.27(9)	108.15(9)	252.9(3)	**4**
$AgRu_2(P_2O_7)_2$	4.7765(8)	6.896(1)	8.069(1)	90.64(1)	92.42(2)	105.55(2)	255.75(5)	**5**
$CuRu_2(P_2O_7)_2$[a)]	(4.799)	(7.043)	(7.950)	(91.18)	(91.96)	(106.98)	(256.71)	**6**
$SrV_2(P_2O_7)_2$	4.8006(7)	7.117(1)	7.8569(8)	89.92(1)	92.38(1)	106.57(1)	257.05(6)	Ref. 5
$NaMo_2(P_2O_7)_2$	4.8813(6)	7.0110(5)	8.2563(4)	91.400(5)	92.466(8)	106.551(9)	270.40(4)	Ref. 3
$NaMo_2(P_2O_7)_2$	4.872(1)	7.0025(7)	8.2620(6)	91.468(8)	92.53(1)	106.61(1)	269.63(6)	Ref. 4

a) These compounds did not well crystallized and the refined cell constants are approximate values.

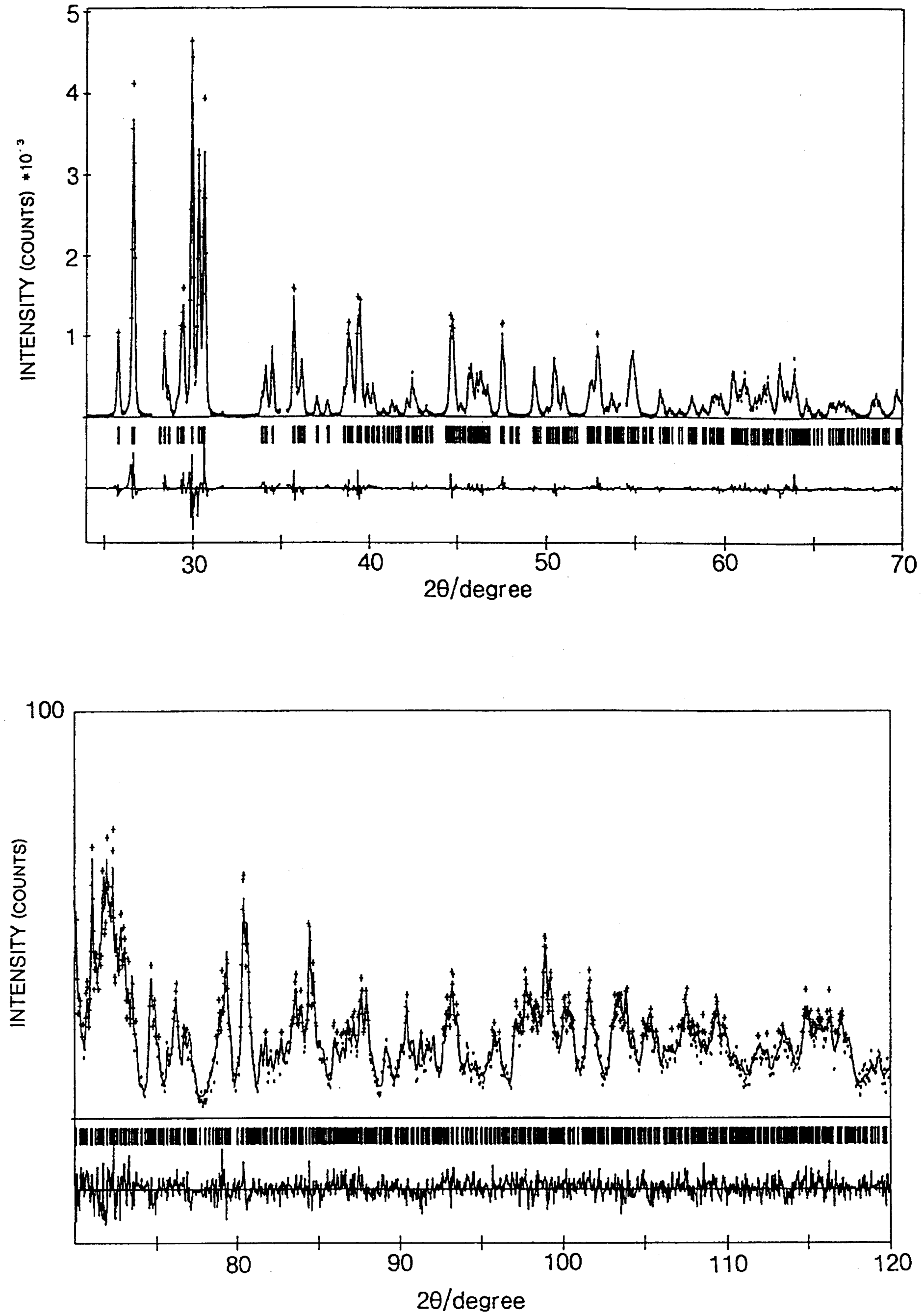

Fig. 1. The result of the Rietveld analysis of $NaRu_2(P_2O_7)_2$ (**2**). The cross marks represent observed intensities, and the solid line represents calculated intensities. The stick marks show the reflection positions. The solid line of the bottom of the figure indicates the difference between the observed and calculated intensities.

are only 0.5 Å apart from the inversion center on the *a*-axis. The ions are randomly distributed in two closely placed positions, and their occupational factors were fixed at 0.5 in the refinement.

Figure 3 shows the magnetic susceptibility ($1/\chi$–T graph) of this compound. They do not obey the Curie–Weiss law, and the effective magnetic moment depends on the temperature. This is mainly due to the spin–orbit coupling effects of Ru^{4+} ions, whose effective magnetic moments depend on the temperature. Since Ru^{3+} and Ru^{4+} ions are well-separated in the structure, we estimated the temperature dependence of the Ru^{4+} and Ru^{3+} ions using the Kotani theory.[12,13] The effective magnetic moments for Ru^{4+} and Ru^{3+} are given by the following equations:

$$\mu_{\mathrm{eff}}^2 = \frac{3\{24+(\frac{\zeta}{2kT}-9)\exp(-\frac{\zeta}{2kT})+(\frac{5\zeta}{2kT}-15)\exp(-\frac{3\zeta}{2kT})\}}{\{1+3\exp(-\frac{\zeta}{2kT})+5\exp(-\frac{3\zeta}{2kT})\}\frac{\zeta}{kT}}$$

for Ru^{4+}, and

$$\mu_{\mathrm{eff}}^2 = \frac{\frac{3\zeta}{kT}+8-8\exp(\frac{-3\zeta}{2kT})}{\{1+2\exp(\frac{-3\zeta}{2kT})\}\frac{\zeta}{kT}}$$

Table 2. Atomic Parameters for $NaRu_2(P_2O_7)_2$ (**2**) with Standard Deviations in Parentheses[a)]

Atom	x	y	z	B
Na	−0.436(5)	0.000(3)	−0.026(3)	1.7(5)
Ru1	0.5	0.0	0.5	0.31(5)
Ru2	0.0	0.5	0.0	0.31
P1	0.123(1)	0.2389(9)	0.6963(8)	0.62(10)
P2	0.540(2)	0.6333(9)	0.7612(8)	0.62
O1	0.384(3)	0.183(2)	0.342(2)	0.52(12)
O2	0.807(3)	0.566(2)	0.787(2)	0.52
O3	0.393(3)	0.665(2)	0.916(2)	0.52
O4	0.990(3)	0.749(2)	0.123(2)	0.52
O5	0.120(3)	0.797(2)	0.440(2)	0.52
O6	0.312(3)	0.102(2)	0.687(2)	0.52
O7	−0.314(3)	0.540(2)	0.352(2)	0.52

a) Reliability factors are as follows. $R_{wp} = 11.74\%$, $R_p = 8.83\%$, $R_R = 10.12\%$, $R_E = 7.43\%$, $R_I = 1.61\%$, $R_F = 0.80\%$.

Table 3. Selected Interatomic Distances for $NaRu_2(P_2O_7)_2$ (**2**)

Ru1–O1	×2	1.980(16) Å	Ru2–O2	×2	2.016(14) Å
–O5	×2	1.988(14)	–O3	×2	2.043(12)
–O6	×2	1.981(14)	–O4	×2	1.988(14)
Na–O1		2.83(3)	Na–O4		3.25(3)
–O1		3.40(3)	–O4		2.49(3)
–O3		2.28(3)	–O6		2.88(3)
–O3		2.43(3)	–O6		2.73(3)
–O4		3.64(3)			

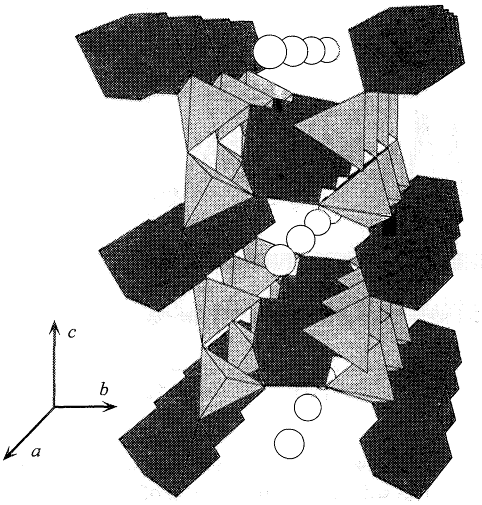

Fig. 2. The structure of $NaRu_2(P_2O_7)_2$ (**2**) illustrating the tunnels running along the a-axis. The octahedra show RuO_6 and tetrahedra show PO_4 units. Open circles indicate Na^+ ions.

for Ru^{3+}.

The spin-coupling constants (ζ) used here were 1180 cm^{-1} for Ru^{3+} and 1350 cm^{-1} for Ru^{4+}, respectively.[14)] The ratio $Ru^{3+} : Ru^{4+}$ was fixed at 1 : 1 in this calculation. As presented in Fig. 3, the observed $1/\chi$ values agree with the calculated curve below 20 K, but deviates in the higher temperature region. An antiferromagnetic transition was observed at around 5.5 K.

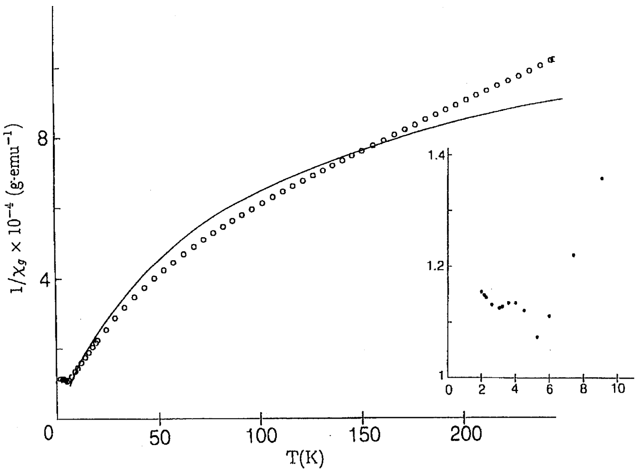

Fig. 3. Inverse of the magnetic susceptibility of $NaRu_2(P_2O_7)_2$ (**2**). The values calculated from Kotani's theory are shown by the solid curve.

Single Crystal of $Na_{0.88}Ru_{1.75}(P_2O_7)_2$ (3). Details of the single crystal analysis of **3** are listed in Tables 4, 5, and 6. The structural analysis has shown that crystal **3** is isotypic with the powder sample **2**, but has some ruthenium and sodium deficiencies. The cell volume of **3** is 4.6 Å^3 (1.8%) smaller than that of **2**. The composition of **3**, calculated from the results of the refinements was $Na_{0.88}Ru_{1.75}(P_2O_7)_2$, and the oxidation state of ruthenium was estimated to be +4.1. Although a small deficiency of sodium was detected in the refinement, it is difficult to determine accurate values of the deficiency based on X-ray diffraction.

Figure 4 shows a projection of the crystal along the tunnel direction (a-axis). There are two crystallographic sites for ruthenium. Ru1 has six diphosphate ions around it. On the other hand, Ru2 is surrounded by four diphosphate groups; two of them are "chelating" ligands, making a trans arrangement. These sites are very different in size. While the average bond distance for Ru1–O is 1.91 Å, the average for

Table 4. Crystallographic Data for $Na_{0.88}Ru_{1.75}(P_2O_7)_2$ (**3**)

Space group	$P\bar{1}$ (No.2)
a (Å)	4.7384(8)
b (Å)	6.8417(10)
c (Å)	7.9526(26)
α (°)	90.72(2)
β (°)	92.74(2)
γ (°)	105.60(1)
V (Å^3)	247.95(10)
Z	1
T (K) of data collection	295
Crystal size (mm)	0.07 × 0.05 × 0.02
2θ limit	$5° \leq 2\theta \leq 60°$
No. of observed reflections with $\lvert F_o \rvert > 3\sigma(\lvert F_o \rvert)$	1624
No. of unique reflections	1051
No. of variable parameters	106
R, R_w[a)]	0.0582, 0.0501

a) $R=\sum(\lvert\lvert F_o\rvert-\lvert F_c\rvert\rvert)/\sum\lvert F_o\rvert$, $R_w=[\sum w(\lvert F_o\rvert-\lvert F_c\rvert)^2/\sum wF_o^2]^{1/2}$ ($w=1/\sigma(F_o)^2$).

Table 5. Atomic Parameters for $Na_{0.88}Ru_{1.75}(P_2O_7)_2$ (**3**) with Standard Deviations in Parentheses

Atom	x	y	z	U_{eq} (Å^2)	Ocp
Na	−0.408(4)	0.004(4)	0.001(4)	0.061(9)	0.44(1)
Ru1	0.5	0.0	0.5	0.0066(7)	0.804(6)
Ru2	0.0	0.5	0.0	0.0080(6)	0.950(8)
P1	0.1134(6)	0.2383(4)	0.6928(3)	0.0108(11)	1.0
P2	0.5200(6)	0.6300(4)	0.7543(3)	0.0105(11)	1.0
O1	0.618(2)	0.8140(10)	0.6474(9)	0.019(3)	1.0
O2	0.218(2)	0.4505(12)	0.2032(9)	0.024(4)	1.0
O3	0.634(2)	0.3239(10)	0.0928(9)	0.015(3)	1.0
O4	0.030(2)	0.2432(10)	0.8735(9)	0.016(3)	1.0
O5	0.861(2)	0.1927(10)	0.5606(9)	0.016(3)	1.0
O6	0.314(2)	0.0936(10)	0.6836(9)	0.016(3)	1.0
O7	0.296(2)	0.4596(10)	0.6419(9)	0.012(3)	1.0

Table 6. Selected Interatomic Distances for $Na_{0.88}Ru_{1.75}(P_2O_7)_2$ (**3**)

Ru1–O1	×2	1.914(7) Å	Ru2–O2	×2	1.959(8) Å
–O5	×2	1.895(7)	–O3	×2	2.006(7)
–O6	×2	1.930(7)	–O4	×2	2.055(7)
P1–O4		1.511(7)	P2–O1		1.508(7)
–O5		1.517(7)	–O2		1.513(8)
–O6		1.548(8)	–O3		1.520(7)
–O7		1.597(7)	–O7		1.582(7)
Na–O3		2.31(2)	Na–O6		2.94(3)
–O3#		2.25(2)	–O6#		2.66(3)
–O4		2.93(3)			
–O4#		2.54(2)	#: $-x, -y, -z$		

Angle (P1–O7–P2)=129.0(3)°.

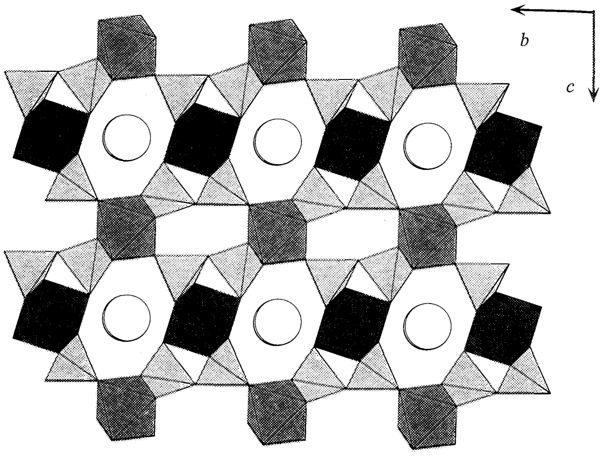

Fig. 4. The projected structure of $Na_{0.88}Ru_{1.75}(P_2O_7)_2$ along the a-axis. Light and dark gray octahedra indicate $Ru1O_6$ and $Ru2O_6$, respectively.

Ru2–O is 2.01 Å.

The local structure of sodium ions and surrounding oxygen atoms are illustrated in Fig. 5. Sodium ions are dislocated from the inversion center and disordered in the two positions. The figure shows only one position of the sodium ion for a simplification. The sodium ion has six nearest oxygen atoms within 3 Å, and four more within 3.8 Å. These ten atoms form a large cage. This cage is connected with the next cages to form the wall of a tunnel whose bottleneck size is about 4.4 Å.

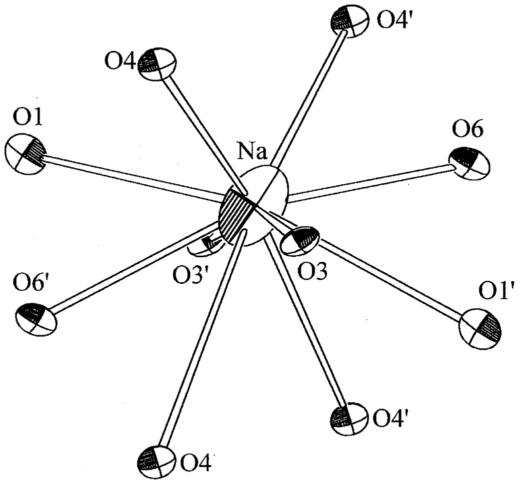

Fig. 5. An ORTEP drawing of a NaO_{10} polyhedron. The sodium ion is enclosed with ten oxygen atoms forming a polyhedral cage. The cage is linearly connected with other cages by sharing O7 oxygen atoms and forms a tunnel running along the a-axis.

As discussed above, the sodium–ruthenium–phosphate system gave two products. One was obtained as a powder sample, and had no ruthenium vacancy. The other was a minor product of the reaction in a sealed tube, and contained a ruthenium vacancy (single-crystal sample). This shows the nonstoichiometry of this system owing to the ruthenium defect.

Comparison of Cell Volumes of $ARu_2(P_2O_7)_2$ A=Li, Ag, Cu, and [ ]. The lattice parameters and cell volumes of **2**—**7** are listed in Table 1. Compound **7** is the end member (x=1) of the $A_{1-x}Ru_2(P_2O_7)_2$ system. It has no cation in the tunnel and has the smallest cell volume. Compound **3** with some ruthenium deficiency has the next smallest volume among them. The cell volume of **5** (A=Ag) is larger than that of **2** (A=Na) and **4** (A=Li), which corresponds to the larger ionic radius of Ag^+. Compound **6** has the largest volume, although the ionic radius of Cu^{2+} is smaller than that of Li^+. A plausible reason is that the copper analog contains only Ru^{3+}, which has a larger ionic radius than Ru^{4+}. The silver analog is a mixed-valence compound of Ru^{3+} and Ru^{4+}.

Isotypic compounds containing other transition metals are reported.[3—5] In the vanadium system, a strontium analog is obtained and the oxidation state of vanadium is +3. It was mentioned without details that the calcium analog was isotypic with the strontium analog.[15] The barium–vanadium system, however, yielded another triclinic phosphate having a different structure with the same composition.[15] The ruthenium system is, therefore, a rare one which has many isotypic members with many kinds of cations.

Conclusion. The chemistry of ruthenium phosphate is very limited because ruthenium is always in the trivalent state in phosphates. However, the present study has revealed that this apparent barrier is not intrinsic to the nature of ruthenium. A suitable choice of the starting compound has led to the preparations of diphosphates containing tetravalent ruthenium. The addition of monovalent or divalent cations gives a series of isotypic diphosphates with a tunnel structure. These findings suggest that further developments of the preparative methods will expand the variety of ruthenium phosphates.

The authors are grateful to Professor T. Iwamoto of the University of Tokyo and Dr. T. Soma of Kitazato University for the powder X-ray diffraction measurements. The authors thank Mr. M. Sakai and the Instrument Center, Institute for Molecular Science, for the use of a magnetic balance. We thank Dr. F. Izumi of National Institute for Research in Inorganic Materials for his program RIETAN. The present work was supported by a Grant-in-Aid for Scientific Research No. 4455 (1996) for H. F. from the Ministry of Education, Science, Sports, and Culture.

References

1) H. Fukuoka, H. Imoto, and T. Saito, *J. Solid State Chem.*, **119**, 107 (1995).

2) H. Fukuoka, H. Imoto, and T. Saito, *J. Solid State Chem.*, **121**, 247 (1996).

3) A. Leclaire, M. M. Borel, A. Grandin, and B. Raveau, *Z. Kristallogr.*, **184**, 247 (1988).

4) K. H. Lii, J. J. Chen, and S. L. Wang, *J. Solid State Chem.*, **78**, 178 (1989).

5) S.-J. Hwu and E. D. Willis, *J. Solid State Chem.*, **93**, 69 (1991).

6) F. Izumi, in "The Rietveld Method," ed by R. A. Young, Oxford Univ. Press, London (1993), Chap. 13.

7) A. C. T. North, D. C. Phillips, and F. S. Mathews, *Acta Crystallogr., Sect. A*, **A24**, 351 (1968).

8) H. Imoto, S. Hayakawa, N. Morita, and T. Saito, *Inorg. Chem.*, **29**, 2007 (1990).

9) K. Kimura and S. Bandow, *Kotai Buturi*, **19**, 467 (1984).

10) W. Klemm, *Z. Anorg. Allg. Chem.*, **244**, 377 (1940).

11) E. König, "Landort-Börnstein, New Series," II/2, Chap. 1 (1966).

12) M. Kotani, *J. Phys. Soc. Jpn.*, **4**, 293 (1949).

13) M. Kotani, *Suppl. Prog. Theor. Phys.*, **14**, 1 (1960).

14) T. M. Dunn, *Trans. Faraday Soc.*, **57**, 1441 (1961).

15) S. J. Hwu, R. I. Carroll, and D. L. Serra, *J. Solid State Chem.*, **110**, 290 (1994).